

Maintaining Strong r -Robustness in Reconfigurable Multi-Robot Networks using Control Barrier Functions

Haejoon Lee¹ and Dimitra Panagou^{1,2}

Abstract—In leader-follower consensus, strong r -robustness of the communication graph provides a sufficient condition for followers to achieve consensus in the presence of misbehaving agents. Previous studies have assumed that robots can form and/or switch between predetermined network topologies with known robustness properties. However, robots with distance-based communication models may not be able to achieve these topologies while moving through spatially constrained environments, such as narrow corridors, to complete their objectives. This paper introduces a Control Barrier Function (CBF) that ensures robots maintain strong r -robustness of their communication graph above a certain threshold without maintaining any fixed topologies. Our CBF directly addresses robustness, allowing robots to have flexible reconfigurable network structure while navigating to achieve their objectives. The efficacy of our method is tested through various simulation and hardware experiments [code]^a.

I. INTRODUCTION

Multi-robot systems are used in tasks such as formation control, search and rescue, and object tracking [1]–[3]. One fundamental algorithm in these tasks is consensus, which enables agents to reach agreement on a common state value. Consensus can be categorized into leaderless consensus and leader-follower consensus. Leaderless consensus aims for all agents to agree on the same state value, whereas leader-follower consensus involves a subset of agents, known as followers, converging to the reference state value propagated by the set of other agents, known as leaders [4]–[8]. In this paper, we focus on the leader-follower consensus.

Consensus in general suffers performance degradation when misbehaving or compromised agents share incorrect, or even adversarial, information, motivating the study of resilient consensus [6], [8]–[14]. The *Weighted Mean-Subsequence-Reduced* (W-MSR) algorithm was introduced to allow the non-compromised (often called normal) agents reach consensus despite the presence of compromised agents [9]. Then [15] showed that resilient leader-follower consensus with misbehaving agents can be achieved using W-MSR under a topological condition called strong r -robustness [13]. A similar property, namely r leader-follower robustness, has been introduced in [8], which, however, requires a trustworthy leader. In this paper, we focus on strong r -robustness.

One common challenge in the literature of resilient leader-follower consensus is the assumption that the agents can pre-

serve and/or switch between predetermined graph topologies with known robustness properties. However, these topologies may not be achievable as robots with distance-based communication models navigate spatially constrained environments. The problem of forming network resilience for leaderless consensus without fixed topologies has been studied in [16]–[18]. However, these focus on r -robustness [9], which is not sufficient for resilient leader-follower consensus and does not directly extend to strong r -robustness [8], [15], [19]. Our paper employs Control Barrier Functions to ensure that robots maintain strong r -robustness above some threshold.

Control Barrier Functions (CBFs) have become a popular technique for enforcing safety while considering desired objectives [20]–[24]. High-order CBFs (HOCBFs) [25] handle constraints with higher relative degrees with respect to system dynamics, and learning-based CBFs have been studied in [26]–[28]. While CBFs have been applied to form resilient multi-robot networks for leaderless consensus in [16], [18], these methods all focus on r -robustness and thus may not extend to resilient leader-follower consensus. In [16], r -robustness of a multi-robot network was controlled indirectly by controlling its algebraic connectivity, which could result in overly conservative formations with unnecessary edges. Authors in [18] focus on forming a specific class of r -robust graph. In contrast, our proposed CBF not only directly addresses strong r -robustness but also assumes no fixed class of graphs, offering a more flexible and general approach.

Contributions: We present a CBF that maintains strong r -robustness of a multi-robot network to ensure resilient leader-follower consensus. We first construct HOCBFs that altogether encode strong r -robustness without maintaining predetermined topologies. These HOCBFs are then composed into a single valid CBF. Finally, we demonstrate the efficacy of our work with numerical and hardware experiments.

Organization: Section II presents the utilized notation. Section III provides the preliminaries and problem statement. HOCBFs for robustness maintenance are constructed in Section IV, and the composed CBF is developed in Section V. The experiment results are presented in Section VI, while conclusion is stated in Section VII.

II. NOTATION

Let $\mathcal{G}(t) = (\mathcal{V}, \mathcal{E}(t))$ be a connected, undirected graph with a vertex set $\mathcal{V} = \{1, \dots, n\}$ and time-varying edge set $\mathcal{E}(t) \subseteq \mathcal{V} \times \mathcal{V}$. Since $\mathcal{G}(t)$ is undirected, an edge $(i, j) \in \mathcal{E}(t)$ implies $(j, i) \in \mathcal{E}(t)$ at the same t . A neighbor set of a node $i \in \mathcal{V}$ at time t is denoted as $\mathcal{N}_i(t) = \{j | (i, j) \in \mathcal{E}(t)\}$. For simplicity, we omit t when the context is clear.

*This work was supported by the Air Force Office of Scientific Research (AFOSR) under Award No. FA9550-23-1-0163.

¹Department of Robotics, University of Michigan, Ann Arbor, MI, USA
haejoonl@umich.edu

²Department of Aerospace Engineering, University of Michigan, Ann Arbor, MI, USA
dpanagou@umich.edu

^a<https://github.com/joonlee16/Resilient-Leader-Follower-CBF-QP>

The set of integers $\{1, \dots, c\}$ is denoted as $[c]$. We denote the cardinality of a set \mathcal{S} as $|\mathcal{S}|$. The set of non-negative integers, positive integers, non-negative reals, and positive reals are denoted as $\mathbb{Z}_{\geq 0}$, \mathbb{Z}_+ , $\mathbb{R}_{\geq 0}$, and \mathbb{R}_+ respectively. Let $\|\cdot\|: \mathbb{R}^m \rightarrow \mathbb{R}_{\geq 0}$ be the Euclidean norm. A $m \times 1$ column vector of 1 and 0 are denoted as $\mathbf{1}_m$ and $\mathbf{0}_m$ respectively. Similarly, a $m \times n$ matrix of 0 are denoted as $\mathbf{0}_{m \times n}$, and an identity matrix of size m is denoted as \mathbf{I}_m . An i^{th} element of $\mathbf{y} \in \mathbb{R}^n$ is denoted as y_i . For $\mathbf{y}, \mathbf{z} \in \mathbb{R}^n$, $\mathbf{y} \geq \mathbf{z}$ or $\mathbf{y} > \mathbf{z}$ means $y_i \geq z_i$ or $y_i > z_i \forall i \in [n]$. We define the Heaviside step function $H: \mathbb{R} \rightarrow \mathbb{R}$ and parametrized sigmoid function $\sigma_{s,q}: \mathbb{R} \rightarrow \mathbb{R}$ with $s \in \mathbb{R}_+$ and $q \in (0, 1)$, respectively:

$$H(y) = \begin{cases} 1 & \text{if } y \geq 0 \\ 0 & \text{otherwise} \end{cases}, \quad (1)$$

$$\sigma_{s,q}(y) = \frac{1+q}{1+q^{-1}e^{-sy}} - q. \quad (2)$$

Note (2) is designed such that i) $\sigma_{s,q}(y) = 0$ when $y = 0$, ii) $\sigma_{s,q}(y) > 0$ when $y > 0$, and iii) $\sigma_{s,q}(y) < 0$ when $y < 0$. Then, we define $H^n: \mathbb{R}^n \rightarrow \mathbb{R}^n$ and $\sigma_{s,q}^n: \mathbb{R}^n \rightarrow \mathbb{R}^n$ as element-wise operations of H and $\sigma_{s,q}$ respectively.

III. PRELIMINARIES AND PROBLEM STATEMENT

A. System Dynamics

We consider a multi-robot system, in which robot i has a physical state represented as $x_i(t) = [p_i(t)^T \ v_i(t)^T]^T \in \mathbb{R}^{2m}$ with position $p_i(t) = [p_{i1} \dots p_{im}]^T \in \mathbb{R}^m$ and velocity $v_i(t) = [v_{i1} \dots v_{im}]^T \in \mathbb{R}^m$. An agent i has double integrator dynamics of the form:

$$\dot{x}_i(t) = \mathbf{A}_i x_i(t) + \mathbf{B}_i u_i(t), \quad (3)$$

where $\mathbf{A}_i = \begin{bmatrix} \mathbf{0}_{m \times m} & \mathbf{I}_m \\ \mathbf{0}_{m \times m} & \mathbf{0}_{m \times m} \end{bmatrix}$, $\mathbf{B}_i = \begin{bmatrix} \mathbf{0}_{m \times m} \\ \mathbf{I}_m \end{bmatrix}$, $u_i(t) \in U_i \subseteq \mathbb{R}^m$ is the control input of a robot i , with U_i being the input constraint set. Let $M = nm$. We denote collective states and control inputs of n robots as $\mathbf{x}(t) = [x_1^T(t) \dots x_n^T(t)]^T \in \mathbb{R}^{2M}$ and $\mathbf{u}(t) = [u_1^T(t) \dots u_n^T(t)]^T \in U = U_1 \times \dots \times U_n \subseteq \mathbb{R}^M$. Also, let $\mathbf{p}(t) = [p_1^T(t), \dots, p_n^T(t)]^T \in \mathbb{R}^M$ and $\mathbf{v}(t) = [v_1^T(t), \dots, v_n^T(t)]^T \in \mathbb{R}^M$. We drop the argument t when context is clear. Thus the full system dynamics is

$$\dot{\mathbf{x}} = \mathbf{A}\mathbf{x} + \mathbf{B}\mathbf{u}, \quad (4)$$

where $\mathbf{A} = \text{diag}([\mathbf{A}_1 \dots \mathbf{A}_n])$ and $\mathbf{B} = \text{diag}([\mathbf{B}_1 \dots \mathbf{B}_n])$.

We now define the robots' communication graph $\mathcal{G}(t) = (\mathcal{V}, \mathcal{E}(t))$ with $\mathbf{x}(t)$ at each t , where $\mathcal{V} = [n]$ represents the robots and $\mathcal{E}(t)$ represents links between two robots. Let $\Delta_{ij}(\mathbf{x}(t)) = \|p_i(t) - p_j(t)\|$ be the distance between robots i and j at time t . We consider a distance-based model

$$\mathcal{E}(t) = \{(i, j) \mid \Delta_{ij}(\mathbf{x}(t)) < R\}, \quad (5)$$

where $R > 0$ is the communication range of robots. The adjacency matrix $A(\mathbf{x}(t))$ of $\mathcal{G}(t)$ has an entry defined as

$$a_{ij}(\mathbf{x}(t)) = \begin{cases} 1 & \text{if } \Delta_{ij}(\mathbf{x}(t)) < R \\ 0 & \text{otherwise} \end{cases}. \quad (6)$$

B. Fundamentals of Strong r -robustness and W-MSR

Consider a connected network $\mathcal{G}(t) = (\mathcal{V}, \mathcal{E}(t))$ where \mathcal{V} is partitioned into two static subsets: leaders $\mathcal{L} \subset \mathcal{V}$ that propagate the same reference value $f_l \in \mathbb{R}$ to followers $\mathcal{F} = \mathcal{V} \setminus \mathcal{L}$. We denote $|\mathcal{L}| = l$ and $|\mathcal{F}| = f$. At discrete times $t_N = N\tau$ for $N \in \mathbb{Z}_{\geq 0}$ where $\tau \in \mathbb{R}_+$ is the update interval, agent i shares its consensus value $y_i(t_N) \in \mathbb{R}$ with its neighbors. Robots have $y(t) = y(t_N) \forall t \in [t_N, t_{N+1})$, and update with

$$y_i(t_{N+1}) = \begin{cases} f_l, & i \in \mathcal{L}, \\ \sum_{j \in \mathcal{N}_i \cup \{i\}} w_{ij}(t_N) y_j(t_N), & i \in \mathcal{F}, \end{cases} \quad (7)$$

where $w_{ij}(t_N)$ is the weight assigned to $y_j(t_N)$ by agent i . We assume $\exists \alpha \in (0, 1)$ such that $\forall i \in \mathcal{V} \forall N \in \mathbb{Z}_{\geq 0}$,

- $w_{ij}(t_N) \geq \alpha$ if $j \in \mathcal{N}_i \cup \{i\}$, or $w_{ij}(t_N) = 0$ otherwise,
- $\sum_{j=1}^n w_{ij}(t_N) = 1$.

Since \mathcal{G} is connected, leader-follower consensus is guaranteed through (7) [29]. However, this guarantee no longer holds with misbehaving agents [15]. Among various models for misbehaving agents, we adopt one below for this paper:

Definition 1 (malicious agent): An agent $i \in \mathcal{V}$ is **malicious** if it sends $y_i(t_N)$ to $\forall j \in \mathcal{N}_i(t_N)$ at time t_N but does not update $y_i(t_{N+1})$ according to (7) at some t_{N+1} [9].

Normal agents are those who are not malicious. Various threat scopes exist to describe the number of malicious agents in a network [9], but for this paper we define one below:

Definition 2 (F-local): A set $\mathcal{S} \subset \mathcal{V}$ is **F-local** if it contains at most F nodes as neighbors of other nodes, i.e., $|\mathcal{N}_i \cap \mathcal{S}| \leq F, \forall i \in \mathcal{V} \setminus \mathcal{S}$ [9].

In [9], W-MSR was introduced to guarantee leaderless consensus with up to F -local malicious agents by having each normal agent i apply the nominal update protocol after discarding up to the F highest and lowest values strictly greater and smaller than its own value $y_i(t)$ at t . Then, [15] showed that leader-follower consensus can be achieved through W-MSR, under a topological property defined below:

Definition 3 (r-reachable [9]): Let $\mathcal{G}(t) = (\mathcal{V}, \mathcal{E}(t))$ be a graph at time t and \mathcal{S} be a nonempty subset of \mathcal{V} . The subset \mathcal{S} is **r-reachable** at t if $\exists i \in \mathcal{S}$ such that $|\mathcal{N}_i(t) \setminus \mathcal{S}| \geq r$.

Definition 4 (strongly r-robust [13]): A graph $\mathcal{G}(t) = (\mathcal{V}, \mathcal{E}(t))$ is **strongly r-robust** with respect to $\mathcal{S}_1 \subset \mathcal{V}$ at time t if $\forall \mathcal{S}_2 \subset \mathcal{V} \setminus \mathcal{S}_1$ such that $\mathcal{S}_2 \neq \emptyset$, \mathcal{S}_2 is r -reachable.

If a network is strongly $(2F+1)$ -robust $\forall t \in \mathbb{R}_{\geq 0}$, normal followers are guaranteed to reach consensus to f_l through W-MSR with up to F -local malicious agents [4].

C. Problem Statement

Let $\mathcal{G}(t_0) = (\mathcal{V}, \mathcal{E}(t_0))$ be a communication graph formed by a system of n robots described by (4) with state $\mathbf{x}(t_0)$ at the initial time $t_0 \in \mathbb{R}_{\geq 0}$. Let $\mathcal{G}(t_0)$ be at least strongly r -robust where $1 \leq r \leq l-1$, and consider the desired control input $\mathbf{u}_{\text{des}} = [u_{1,\text{des}}^T \dots u_{n,\text{des}}^T]^T$. We aim to design a control strategy so that the network remains at least strongly r -robust while minimally deviating from $\mathbf{u}_{\text{des}}(t) \forall t \geq t_0$.

To solve this, we use High Order Control Barrier Functions (HOCBFs) [25] and Bootstrap Percolation (BP) [30]. Before presenting the solution in Section V, we first describe these concepts in the remainder of the section.

D. High-Order Control Barrier Function

We first present High Order Control Barrier Functions (HOCBFs), which are introduced in [25]. Note in this paper, we are considering time-invariant HOCBFs. Let d^{th} order differentiable function $h : \mathcal{D} \subset \mathbb{R}^{2M} \rightarrow \mathbb{R}$ have a relative degree d with respect to system (4). We define $\psi_0 := h(\mathbf{x})$ and a series of functions $\psi_i : \mathcal{D} \rightarrow \mathbb{R}$, $i \in [d]$, as

$$\psi_i(\mathbf{x}) := \dot{\psi}_{i-1}(\mathbf{x}) + \alpha_i(\psi_{i-1}(\mathbf{x})), \quad i \in [d], \quad (8)$$

where $\alpha_i(\cdot)$ are class \mathcal{K} functions, and $\dot{\psi}_i(\mathbf{x}) = \frac{\partial \psi_i}{\partial \mathbf{x}}(\mathbf{A}\mathbf{x} + \mathbf{B}\mathbf{u})$. Each function ψ_i defines a set \mathcal{C}_i as follows:

$$\mathcal{C}_i := \{\mathbf{x} \in \mathbb{R}^{2M} \mid \psi_{i-1}(\mathbf{x}) \geq 0\}, \quad i \in [d]. \quad (9)$$

Let $\mathcal{C} = \bigcap_{i=1}^d \mathcal{C}_i$. Now, we formally define HOCBF:

Definition 5 (HOCBF [25]): Let $\psi_i(\mathbf{x})$, $i \in \{0, \dots, d\}$, be defined by (8) and \mathcal{C}_i , $i \in [d]$, be defined by (9). Then, a function $h : \mathcal{D} \rightarrow \mathbb{R}$ is a **HOCBF** of relative degree d for system (4) if there exist differentiable class \mathcal{K} functions $\alpha_1, \dots, \alpha_d$ such that

$$\sup_{\mathbf{u} \in U} [\psi_d(\mathbf{x})] \geq 0, \quad \forall \mathbf{x} \in \mathcal{C}. \quad (10)$$

Theorem 1: Given the HOCBF h and its safety set \mathcal{C} , if $x(t_0) \in \mathcal{C}$, any Lipschitz continuous controller $\mathbf{u}(\mathbf{x}) \in K_{\text{hocbf}}(\mathbf{x}) = \{\mathbf{u} \in U \mid \psi_d(\mathbf{x}) \geq 0\}$ renders \mathcal{C} forward invariant for system (4) [25].

HOCBF is a generalization of Control Barrier Function (CBF) with $d = 1$ [20], [21], [25]. In this paper, we present a CBF that enforces multi-robot system to form strongly r -robust network, where $r \in \mathbb{Z}_+$ is a user-given parameter.

E. Bootstrap Percolation

Now, we introduce bootstrap percolation (BP) [30]. Let $\mathcal{G}(t) = (\mathcal{V}, \mathcal{E}(t))$ be a communication graph formed by n robots with physical states $\mathbf{x}(t)$ at time t . Given user-defined threshold $r \in \mathbb{Z}_+$ and initial set of active nodes $\mathcal{L} = [l] \subset \mathcal{V}$, BP models the spread of *activation* of nodes of \mathcal{G} from \mathcal{L} . In BP, each node is either *active* (activation state 1) or *inactive* (activation state 0). The process iteratively activates nodes with at least r active neighbors until no further activations occur, terminating in at most $|\mathcal{F}| = f$ iterations. Once activated, a node stays active until termination. If all nodes in \mathcal{V} become active through BP with threshold r and initial active set \mathcal{L} , then we say \mathcal{L} percolates \mathcal{G} with threshold r .

We now mathematically define the process of BP up to a given number of iterations δ where $1 \leq \delta \leq f$. Let $\pi_j^r(k)$ denote the activation state of node j at iteration $k \in \{0, \dots, \delta\}$ of BP, which is updated using the rule below

$$\pi_j^r(k+1) = \begin{cases} 1 & \text{if } \pi_j^r(k) = 1 \\ 1 & \text{if } \sum_{i \in \mathcal{N}_j} \pi_i^r(k) \geq r \\ 0 & \text{if } \sum_{i \in \mathcal{N}_j} \pi_i^r(k) < r \end{cases} \quad (11)$$

We now define an activation state vector of all nodes at iteration k as $\pi^r(k) = [\pi_1^r(k) \cdots \pi_n^r(k)]^T$. This can be decomposed into $\pi^r(k) = [\pi_{\mathcal{L}}^r(k)^T \quad \pi_{\mathcal{F}}^r(k)^T]^T$, where $\pi_{\mathcal{L}}^r(k) = [\pi_1^r(k) \cdots \pi_l^r(k)]^T$ and $\pi_{\mathcal{F}}^r(k) = [\pi_{l+1}^r(k) \cdots \pi_n^r(k)]^T$ are activation state vectors of leaders and followers at iteration

k , respectively. Then, $\pi_{\mathcal{L}}^r(0) = \mathbf{1}_l$ and $\pi_{\mathcal{F}}^r(0) = \mathbf{0}_f$. Note that $\pi^r(\delta) = \mathbf{1}_n$ implies \mathcal{L} percolates \mathcal{G} with threshold r . Now, we present a lemma from [13]:

Lemma 1: Given a graph \mathcal{G} and threshold $r \in \mathbb{Z}_+$, an initial set \mathcal{L} percolates \mathcal{G} with threshold r if and only if \mathcal{G} is strongly r -robust with respect to \mathcal{L} [13].

Using Lemma 1, we derive the following corollary:

Corollary 1: Given a graph \mathcal{G} , threshold $r \in \mathbb{Z}_+$, and initial set \mathcal{L} , the process of BP activates every follower $i \in \mathcal{F}$ if and only if \mathcal{G} is strongly r -robust with respect to \mathcal{L} .

With Corollary 1, $\pi_{\mathcal{F}}^r(\delta) = \mathbf{1}_f$ directly implies that $\mathcal{G}(t)$ is strongly r -robust at time t . We use this intuition to build HOCBFs in the next section.

IV. HOCBFs FOR STRONG r -ROBUSTNESS

Here, we construct HOCBFs that create sufficient connections for a communication graph $\mathcal{G}(t) = (\mathcal{V}, \mathcal{E}(t))$ to be strongly r -robust with respect to its leader set $\mathcal{L} = [l] \subset \mathcal{V}$. Let $\pi^r(k)$ be an activation state vector of all nodes at iteration $k \in \{0, \dots, \delta\}$ of BP where $1 \leq \delta \leq f$. Let $A(\mathbf{x})$ be an adjacency matrix of \mathcal{G} at time t . Using the reasoning of BP, we recursively represent $\pi_{\mathcal{F}}^r(k)$ for $k \in [\delta]$ with $\pi_{\mathcal{F}}^r(0) = \mathbf{0}_f$:

$$\pi_{\mathcal{F}}^r(k) = H^f \left(\underbrace{[\mathbf{0}_{f \times l} \quad \mathbf{I}_f]}_K A(\mathbf{x}) \begin{bmatrix} \mathbf{1}_l \\ \pi_{\mathcal{F}}^r(k-1) \end{bmatrix} - r \mathbf{1}_f \right) \quad (12)$$

where i^{th} element of $K \in \mathbb{R}^f$ indicates how many active neighbors a follower i has at iteration k .

A. Continuous Representation of the Activation States

However, $\pi_{\mathcal{F}}^r(\delta)$ as a result of (12) for $k \in [\delta]$ is not continuous and thus not suitable for HOCBF. Therefore, we construct a smooth approximation of $\pi_{\mathcal{F}}^r(\delta)$. We first define a parameter set $\mathcal{B} = \{s, s_A, q, q_A\}$ where $s, s_A \in \mathbb{R}_+$ and $q, q_A \in (0, 1)$. We also define $\bar{A}(\mathbf{x})$ whose entry is

$$\bar{a}_{ij}(\mathbf{x}) = \begin{cases} \sigma_{s_A, q_A} \left((R^2 - \Delta_{ij}(\mathbf{x})^2)^3 \right) & \text{if } \Delta_{ij}(\mathbf{x}) < R \\ 0 & \text{otherwise} \end{cases} \quad (13)$$

Note that $\bar{a}_{ij}(\mathbf{x}) \rightarrow 1$ as robots i and j get closer in distance, while $\bar{a}_{ij}(\mathbf{x}) \rightarrow 0$ as they get further apart. Also with $\sigma_{s_A, q_A}(0) = 0$ and $(R^2 - \Delta_{ij}(\mathbf{x})^2)^3$, one can verify that it is twice continuously differentiable $\forall \mathbf{x} \in \mathbb{R}^{2M}$. By replacing $A(\mathbf{x})$ and H^f in (12) with $\bar{A}(\mathbf{x})$ and $\sigma_{s, q}^f$, respectively, we construct $\bar{\pi}_{\mathcal{F}}^r(k) = [\bar{\pi}_{l+1}^r(k) \cdots \bar{\pi}_n^r(k)]^T$, $k \in [\delta]$, where

$$\bar{\pi}_{\mathcal{F}}^r(k) = \sigma_{s, q}^f \left([\mathbf{0}_{f \times l} \quad \mathbf{I}_f] \bar{A}(\mathbf{x}) \begin{bmatrix} \mathbf{1}_l \\ \bar{\pi}_{\mathcal{F}}^r(k-1) \end{bmatrix} - r \mathbf{1}_f \right) \quad (14)$$

with $\bar{\pi}_{\mathcal{F}}^r(0) = \mathbf{0}_f$. We now show that $\bar{\pi}_{\mathcal{F}}^r(\delta)$ also gives sufficient information to determine if \mathcal{G} is strongly r -robust.

Lemma 2: Let $n' \in \mathbb{Z}_+$, $s' \in \mathbb{R}_+$, and $q' \in (0, 1)$. Then, $H^{n'}(\mathbf{y}) > \sigma_{s', q'}^{n'}(\mathbf{y}) \forall \mathbf{y} \in \mathbb{R}^{n'}$.

Proof: Since $H^{n'}(\cdot)$ and $\sigma_{s', q'}^{n'}(\cdot)$ are element-wise operations of $H(\cdot)$ and $\sigma_{s', q'}(\cdot)$, we just need to prove $H(y_i) > \sigma_{s', q'}(y_i)$. Dropping the subscript i and superscript $'$, we get $\sigma_{s, q}(y) = \frac{1+q}{1+e^{-sy}(1/q)} - q = \frac{q(1+q)}{q+e^{-sy}} - q = \frac{q(1-e^{-sy})}{q+e^{-sy}}$. We know i) $s \in \mathbb{R}_+$ and ii) $q \in (0, 1)$. Thus,

If $y \geq 0$, $H(y) = 1 > \sigma_{s,q}(y) \geq 0$ as $0 \leq q(1 - e^{-sy}) < q$.

If $y < 0$, $H(y) = 0 > \sigma_{s,q}(y)$ as $e^{-sy} > 1$. ■

Using Lemma 2, we characterize $\bar{\pi}_{\mathcal{F}}^r(\delta)$ in terms of \mathcal{G} 's robustness in the following proposition:

Proposition 1: Let $\mathcal{G}(t) = (\mathcal{V}, \mathcal{E}(t))$ be a communication graph of a system of n robots with states $\mathbf{x}(t)$. Let $\mathcal{L} = [l] \subset \mathcal{V}$ and $\mathcal{F} = \mathcal{V} \setminus \mathcal{L}$ be leader and follower sets. Let $\delta \in \mathbb{Z}_+$ such that $\delta \leq f$. Also, let $\bar{\pi}_{\mathcal{F}}^r(\delta)$ be computed from (14) for $k \in [\delta]$ using $\mathcal{B} = \{s, s_A, q, q_A\}$ with $s, s_A \in \mathbb{R}_+$ and $q, q_A \in (0, 1)$. Then, $\mathcal{G}(t)$ is strongly r -robust with respect to \mathcal{L} at time t if $\bar{\pi}_{\mathcal{F}}^r(\delta) \geq \mathbf{0}_f$.

Proof: Corollary 1 shows that \mathcal{G} is strongly r -robust with respect to \mathcal{L} if $\pi_{\mathcal{F}}^r(\delta) = \mathbf{1}_f$. Now, we compare $\pi_{\mathcal{F}}^r(\delta)$ with $\bar{\pi}_{\mathcal{F}}^r(\delta)$. With Lemma 2, $\bar{a}_{ij}(\cdot)$ defined at (13) always under-approximate $a_{ij}(\cdot)$ defined at (6). Again, with Lemma 2, $\sigma_{s,q}^n(\cdot) < H^n(\cdot)$ for the same argument. Therefore, with $\bar{\pi}_{\mathcal{F}}^r(0) = \pi_{\mathcal{F}}^r(0)$, $\bar{\pi}_{\mathcal{F}}^r(k) < \pi_{\mathcal{F}}^r(k) \forall k \in [\delta - 1]$. Since i) $\bar{\pi}_{\mathcal{F}}^r(\delta - 1) < \pi_{\mathcal{F}}^r(\delta - 1)$ and ii) $H^n(\mathbf{0}_n) = \mathbf{1}_n$ while $\sigma_{s,q}^n(\mathbf{0}_n) = \mathbf{0}_n$, $\bar{\pi}_{\mathcal{F}}^r(\delta) \geq \mathbf{0}_f \rightarrow \pi_{\mathcal{F}}^r(\delta) = \mathbf{1}_f$. ■

Remark 1: Proposition 1 ensures that $\mathcal{G}(t)$ is strongly r -robust with respect to \mathcal{L} if $\bar{\pi}_{\mathcal{F}}^r(\delta) \geq \mathbf{0}_f$, but it also introduces a tradeoff. Since $\bar{a}_{ij}(\cdot) < 1$, with strongly r_0 -robust $\mathcal{G}(t_0)$, $\bar{\pi}_{\mathcal{F}}^r(1) < \mathbf{0}_f$ if $l = r_0$. This means $\bar{\pi}_{\mathcal{F}}^r(\delta) < \mathbf{0}_f$ unless $l > r_0$. Thus, we only consider $r_0 \leq l - 1$ in this paper.

B. HOCBF for Robustness Maintenance

Let $\epsilon \in \mathbb{R}_+$ be a small constant. Using Proposition 1, we construct the following candidate HOCBFs:

$$h_r(\mathbf{x}) = \begin{bmatrix} h_{r,1}(\mathbf{x}) \\ \vdots \\ h_{r,f}(\mathbf{x}) \end{bmatrix} = \begin{bmatrix} \bar{\pi}_{l+1}^r(\delta) - \epsilon \\ \vdots \\ \bar{\pi}_n^r(\delta) - \epsilon \end{bmatrix} = \bar{\pi}_{\mathcal{F}}^r(\delta) - \epsilon \mathbf{1}_f. \quad (15)$$

Note $h_{r,c}(\mathbf{x})$, $c \in [\delta]$, is twice continuously differentiable and has a relative degree 2 to dynamics (4). Thus, we have:

$$\begin{aligned} \psi_{c,0}(\mathbf{x}) &:= h_{r,c}(\mathbf{x}), \\ \psi_{c,1}(\mathbf{x}) &:= \dot{\psi}_{c,0}(\mathbf{x}) + \eta_{c,1}\psi_{c,0}(\mathbf{x}), \\ \psi_{c,2}(\mathbf{x}) &:= \dot{\psi}_{c,1}(\mathbf{x}) + \eta_{c,2}\psi_{c,1}(\mathbf{x}), \end{aligned} \quad (16)$$

where $\eta_{c,1}, \eta_{c,2} \in \mathbb{R}_+$. Let $\mathcal{C}_{c,i} = \{\mathbf{x} \in \mathbb{R}^{2M} \mid \psi_{c,i-1}(\mathbf{x}) \geq 0\}$, $i \in [2]$. When $\mathbf{x} \in \mathcal{C}_c = \bigcap_{i=1}^2 \mathcal{C}_{c,i}$, the agents are arranged so that follower c can maintain sufficient connections to preserve the network's strong r -robustness at time t . Since strong r -robustness requires all agents to be sufficiently connected, we need $\mathbf{x} \in \mathcal{C} = \bigcap_{c=1}^f \mathcal{C}_c$. Also, we aim to maintain the initial level of robustness or one lower, i.e., $\mathbf{x}(t_0) \in \mathcal{C}$. We now assume:

Assumption 1: Inter-agent collision avoidance is enforced.

Assumption 2: The control input is unbounded: $U = \mathbb{R}^M$.

Also, we define an extreme agent, adopting from [31]. Let agent $I \in \mathcal{V}$ with position $p_I = [p_{I1}, \dots, p_{Im}]^T \in \mathbb{R}^m$ be an extreme agent at dimension b if $\exists b \in [m]$ such that $p_{Ib} > p_{jb} \forall j \in \mathcal{V} \setminus \{I\}$ or $p_{Ib} < p_{jb} \forall j \in \mathcal{V} \setminus \{I\}$. In words, extreme agents at dimension b have the strictly largest or smallest b^{th} position component. We assume extreme agents always exist. In fact, under Assumption 1, their absence would

require at least $2m$ agent pairs to have the same position components, which can be easily avoided. We do not address the case formally here. A potential solution is adding small perturbations to a robot's position or defining a different control law for these configurations; fully addressing this limitation remains future work. Now we provide a lemma:

Lemma 3: Let all conditions in Proposition 1 hold. Let $h_r(\mathbf{x})$ (15) be computed with $\mathbf{x} \in \mathcal{C}$. Then, $\exists I \in [n], b \in [m]$ such that $\frac{\partial h_{r,c}}{\partial p_{Ib}}(\mathbf{x}) > 0 \forall c \in [f]$ or $\frac{\partial h_{r,c}}{\partial p_{Ib}}(\mathbf{x}) < 0 \forall c \in [f]$.

Proof: Let $D = \delta - 1$, $c \in [f]$, and $j = c + l$. With $\bar{\pi}_j^r(0) = 0 \forall j \in \mathcal{F}$, we write $\bar{\pi}_j^r(k+1)$, $k \in \{0, \dots, D\}$, as

$$\bar{\pi}_j^r(k+1) = \sigma_{s,q} \left(\underbrace{\sum_{i=1}^l \bar{a}_{ji} + \sum_{i=l+1}^n \bar{a}_{ji} \bar{\pi}_i^r(k)}_{B_{j,k}} - r \right). \quad (17)$$

Considering extreme agent $I \in \mathcal{V}$ at dimension $b \in [m]$, the partial derivative of $h_{r,c}(\mathbf{x})$ with respect to p_{Ib} is

$$\frac{\partial h_{r,c}}{\partial p_{Ib}} = \frac{\partial \sigma_{s,q}}{\partial B_{j,D}} \left(\sum_{i=1}^l \frac{\partial \bar{a}_{ji}}{\partial p_{Ib}} + \sum_{i=l+1}^n \left(\frac{\partial \bar{a}_{ji}}{\partial p_{Ib}} \bar{\pi}_i^r(D) + \bar{a}_{ji} \frac{\partial \bar{\pi}_i^r(D)}{\partial p_{Ib}} \right) \right), \quad (18)$$

where, with $n_{ij}(\mathbf{x}) = [\Delta_{ij}(\mathbf{x})]^2$,

$$\begin{aligned} \frac{\partial \bar{\pi}_i^r(k+1)}{\partial p_{Ib}} &= \frac{\partial \sigma_{s,q}}{\partial B_{i,k}} \left(\sum_{g=1}^l \frac{\partial \bar{a}_{ig}}{\partial p_{Ib}} + \sum_{g=l+1}^n \left(\frac{\partial \bar{a}_{ig}}{\partial p_{Ib}} \bar{\pi}_g^r(k) + \bar{a}_{ig} \frac{\partial \bar{\pi}_g^r(k)}{\partial p_{Ib}} \right) \right), \\ \frac{\partial \bar{a}_{ji}}{\partial p_{Ib}} &= \begin{cases} \frac{\partial \bar{a}_{ji}}{\partial n_{ji}} \frac{\partial n_{ji}}{\partial p_{Ib}} & \text{if } I \in \{i, j\} \\ 0 & \text{otherwise} \end{cases}. \end{aligned} \quad (20)$$

Now we list some facts:

- $\frac{\partial \sigma_{s,q}}{\partial B_{j,D}}(B_{j,D}) > 0$, since $\sigma_{s,q}$ is strictly monotonically increasing and continuously differentiable functions.
- If $I \in \{i, j\}$ and $(i, j) \in \mathcal{E}$, $\frac{\partial \bar{a}_{ji}}{\partial n_{ji}}(\mathbf{x}) > 0$.
- If $I \in \{i, j\}$ and $i \neq j$, $\frac{\partial n_{ji}}{\partial p_{Ib}}(\mathbf{x}) = (\pm 2(p_{jb} - p_{ib})) > 0 \forall i, j \in [n]$ or $\frac{\partial n_{ji}}{\partial p_{Ib}}(\mathbf{x}) < 0 \forall i, j \in [n]$.
- If $D > 1$, $\bar{\pi}_i^r(D) > \epsilon \forall i \in \mathcal{F}$ as $\mathbf{x} \in \mathcal{C}$.

Since $|\mathcal{N}_I| \geq 1$, we can infer that if $I \in \{i, j\}$ and $i \neq j$, $\exists i, j \in \mathcal{V}$ that (20) is nonzero, and the nonzero values are either all positive or negative. If $D = 0$, $\forall j \in \mathcal{F} \exists i \in [l]$ that $\frac{\partial \bar{a}_{ji}}{\partial n_{ji}}(\mathbf{x}) > 0$, so $\frac{\partial h_{r,c}}{\partial p_{Ib}} > 0$ or $\frac{\partial h_{r,c}}{\partial p_{Ib}} < 0 \forall c \in [f]$. If $D > 0$, either $\frac{\partial \bar{\pi}_i^r(k)}{\partial p_{Ib}} > 0 \forall i \in [f] \forall k \in [D]$ or $\frac{\partial \bar{\pi}_i^r(k)}{\partial p_{Ib}} < 0 \forall i \in [f] \forall k \in [D]$. Then, $\forall c \in [f]$ i) (18) has nonzero terms, and ii) all of them for all c have the same sign. ■

Now we use Lemma 3 to validate our HOCBFs:

Theorem 2: Let all conditions in Lemma 3 hold. Also, let $\psi_{c,2}(\mathbf{x})$ be from (16). Then, $h_{r,c}(\mathbf{x})$ is a HOCBF of relative degree 2 for system (4) $\forall c \in [f]$.

Proof: For each $c \in [f]$, we need to show that

$$\sup_{\mathbf{u} \in U} [\psi_{c,2}(\mathbf{x})] \geq 0, \quad \forall \mathbf{x} \in \mathcal{C}, \quad (21)$$

where

$$\psi_{c,2}(\mathbf{x}) = \underbrace{\mathbf{v}^T \frac{\partial^2 h_{r,c}}{\partial \mathbf{p}^2} \mathbf{v} + \frac{\partial h_{r,c}}{\partial \mathbf{p}} \mathbf{u} + \eta_{c,1} \frac{\partial h_{r,c}}{\partial \mathbf{p}} \mathbf{v} + \eta_{c,2} \psi_{c,1}(\mathbf{x})}_{\dot{\psi}_{c,1}(\mathbf{x})}. \quad (22)$$

With Assumption 2, it suffices to show that $\frac{\partial h_{r,c}}{\partial \mathbf{p}}(\mathbf{x}) \neq \mathbf{0}_M^T$ $\forall \mathbf{x} \in \mathcal{C} \forall c \in [f]$, which is given in Lemma 3. ■

Note the HOCBFs (15) are functions of robots' states \mathbf{x} and desirable level of strong r -robustness. They directly consider robustness without imposing maintenance of fixed topologies, allowing robots to have more flexible formations.

V. CBF COMPOSITION

A. Composition of Multiple HOCBFs

Given f HOCBFs (15), we now seek to compose them into one CBF. Composition methods are studied in [32]–[35], and in this paper we use a form inspired by [32]. We define a candidate CBF $\phi_r : \mathbb{R}^{2M} \times \mathbb{R}_+^f \rightarrow \mathbb{R}$ as follows:

$$\phi_r(\mathbf{x}, \mathbf{w}) = 1 - \sum_{c=1}^f e^{-w_c \psi_{c,1}(\mathbf{x})}, \quad (23)$$

where $\mathbf{w} = \{w_c \in \mathbb{R}_+ \mid c \in [f]\} \in \mathbb{R}_+^f$. Its structure implies that $\phi_r(\mathbf{x}, \mathbf{w}) \geq 0$ only when $\psi_{c,1}(\mathbf{x}) \geq 0 \forall c \in [f]$. Then, the safety set $\mathcal{S}(\mathbf{w}) = \{\mathbf{x} \in \mathbb{R}^{2M} \mid \phi_r(\mathbf{x}, \mathbf{w}) \geq 0\} \subset \mathcal{C}$. How close $\mathcal{S}(\mathbf{w})$ gets to \mathcal{C} depends on the values of \mathbf{w} . Note in [32], the values of \mathbf{w} are adjusted to validate their composed CBF. However, due to the nature of our HOCBFs (15), we do not need to adjust them, as shown below:

Theorem 3: Let all conditions in Theorem 2 hold. Let

$$\psi(\mathbf{x}) = [\psi_{1,1}(\mathbf{x}) \quad \cdots \quad \psi_{f,1}(\mathbf{x})] \quad (24)$$

and $\mathbf{w} \in \mathbb{R}_+^f$. Then, (23) is a valid CBF with system (4).

Proof: We know (23) is continuously differentiable and has a relative degree 1 with system (4). Now, we prove:

$$\sup_{\mathbf{u} \in U} \left[\frac{\partial \phi_r}{\partial \mathbf{x}}(\mathbf{A}\mathbf{x} + \mathbf{B}\mathbf{u}) \right] \geq 0, \quad \forall \mathbf{x} \in \mathcal{C}. \quad (25)$$

We can rewrite $\frac{\partial \phi_r}{\partial \mathbf{x}}(\mathbf{A}\mathbf{x} + \mathbf{B}\mathbf{u})$ in (25) as $\frac{\partial \phi_r}{\partial \psi} \dot{\psi}$ where

$$\frac{\partial \phi_r}{\partial \psi}(\mathbf{x}) = [w_1 e^{-w_1 \psi_{1,1}(\mathbf{x})} \quad \cdots \quad w_f e^{-w_f \psi_{f,1}(\mathbf{x})}], \quad (26)$$

$$\dot{\psi}(\mathbf{x}) = [\dot{\psi}_{1,1}(\mathbf{x})^T \quad \cdots \quad \dot{\psi}_{f,1}(\mathbf{x})^T]^T. \quad (27)$$

From (22), the coefficient of the control input \mathbf{u} in $\dot{\psi}$ is $\frac{\partial h_r}{\partial \mathbf{p}}$. Then, with Assumption 2, we just need to show that

$$\frac{\partial \phi_r}{\partial \psi}(\mathbf{x}) \frac{\partial h_r}{\partial \mathbf{p}}(\mathbf{x}) \neq \mathbf{0}_M^T, \quad \forall \mathbf{x} \in \mathcal{S}(\mathbf{w}) \subset \mathcal{C}. \quad (28)$$

Since i) \exists column in $\frac{\partial h_r}{\partial \mathbf{p}}$ where all nonzero entries have the same sign (Lemma 3), and ii) $\frac{\partial \phi_r}{\partial \psi}(\mathbf{x}) > \mathbf{0}_f^T$, (28) holds. ■

Using our CBF (23), the robots can maintain robustness without specific network topologies unlike the assumptions in [4], [8], [12], [15], while minimally deviating from \mathbf{u}_{des} . Note it only takes robots' states and desirable robustness level. This provides robots with flexible reconfigurable network formations such that they deviate from \mathbf{u}_{des} only when their motions conflict with desire to maintain robustness.

VI. EXPERIMENTAL RESULTS

Now we demonstrate our work through simulations and hardware experiments. For practical deployments, we incorporate inter-agent and obstacle collision avoidance into our controller. Modeling robots and obstacles as point masses, robots must maintain distances of at least Δ_d from each other and Δ_o from obstacles. These constraints are encoded as additional CBFs and composed with (23) into a candidate CBF $Y : \mathbb{R}^{2M} \times \mathbb{R}_+^f \rightarrow \mathbb{R}$, which defines a safety set $\mathcal{W} = \{\mathbf{x} \in \mathbb{R}^{2M} \mid Y(\mathbf{x}, \mathbf{w}) \geq 0\} \subset \mathcal{S}(\mathbf{w})$. Note that establishing $Y(\mathbf{x}, \mathbf{w})$ as a valid CBF is an open problem and is not addressed in this paper. We now construct our CBF-based QP (CBF-QP) controller:

$$\begin{aligned} \mathbf{u}(\mathbf{x}) &= \arg \min_{\mathbf{u} \in \mathbb{R}^M} \|\mathbf{u}_{\text{des}} - \mathbf{u}\|^2 \\ \text{s.t. } \frac{\partial Y}{\partial \mathbf{x}}(\mathbf{A}\mathbf{x} + \mathbf{B}\mathbf{u}) &\geq -\alpha_T(Y(\mathbf{x}, \mathbf{w})), \end{aligned} \quad (29)$$

where $\alpha_T(\cdot)$ is a class \mathcal{K} function.

In this setup, robots with states \mathbf{x} form a network using (5) and constantly emit LED colors corresponding to their scalar consensus values in $[0, 1]$. Robots share their values with neighbors every $\tau = 0.5$ seconds. Normal leaders all maintain the same value $f_l \in [0, 1]$ and thus display the same LED color, while normal followers start with random values in $[0, 1]$ and adjust them through W-MSR to match leaders' LED colors (consensus values). Malicious agents randomly choose and share values in $[0, 1]$ every τ seconds, updating their LEDs accordingly. We evaluate efficacy of our CBF by observing whether followers successfully match their LED colors to the normal leaders' LED colors despite malicious agents. We set $\delta = 4$, $\epsilon = 10^{-4}$, $\Delta_d = 0.3$ m, and $\Delta_o \in \{0.4, 0.7\}$ m, based on obstacle sizes. Codes and video are available here¹.

A. Simulation

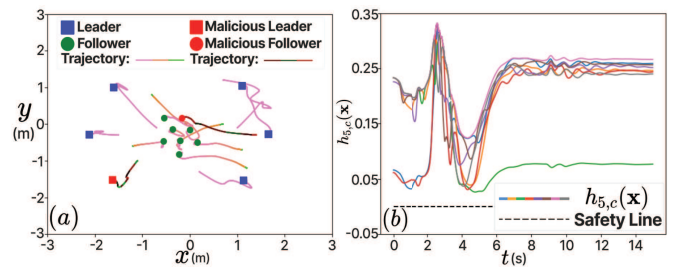


Fig. 1: (a) and (b) display the evolutions of robots' trajectories in their LED colors and $h_5(\mathbf{x})$ (15) from the first simulation, respectively.

1) Spread Out: We show that our CBF can maintain strong r -robustness, even when the desired control input directly conflicts with maintaining the network's robustness. Let $p_{i,\text{goal}}$ be a goal location for agent i . We set \mathbf{u}_{des} as

$$u_{i,\text{des}} \begin{cases} \frac{(p_{i,\text{goal}} - p_i)}{\|p_{i,\text{goal}} - p_i\|} - v_i, & i \in \mathcal{L}, \\ 0, & i \in \mathcal{F}, \end{cases} \quad (30)$$

¹<https://github.com/joonlee16/Resilient-Leader-Follower-CBF-QP>

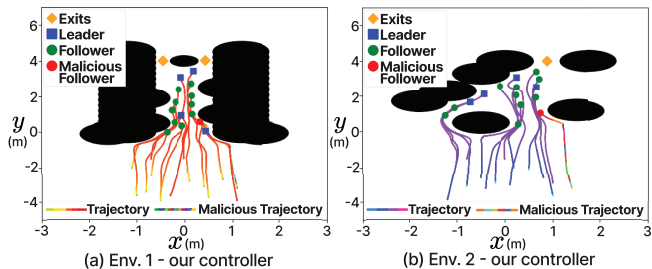


Fig. 2: (a) and (b) show the snapshots of the simulations with our controller and dynamics (4) in Env. 1 and 2, respectively.

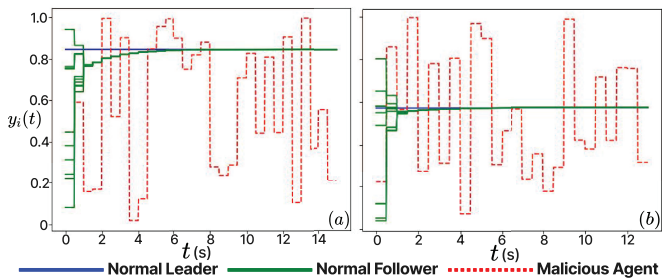


Fig. 3: (a) and (b) show the evolutions of robots' consensus values for the simulations visualized in Fig. 2 (a) and (b), respectively.

where we set $p_{i,\text{goal}}$ such that leaders would spread out in different directions. In the initial setup, we had six leaders (one malicious) and eight followers (one malicious) forming a strongly 6-robust network with a communication range $R = 3$ m. The system aimed to maintain strong 5-robustness to ensure consensus under a 2-local malicious attack. Fig. 1 (a) shows the robots' trajectories colored in their LED colors, while Fig. 1 (b) shows the evolutions of $h_5(\mathbf{x})$ (15). The network remained strongly 5-robust throughout the simulation, and followers successfully matched their LEDs to normal leaders'. Notably, when the network approached losing 5-robustness at around $t = 4$ (Fig. 1 (b)), the leaders stopped dispersal while the followers gathered at the center.

2) Complex Environments: We evaluated our controller in two complex environments visualized in Fig. 2. In the initial setup, four normal leaders and eleven followers (one malicious) formed a strongly 4-robust network with $R = 3$ m. Each robot i had $u_{i,\text{des}} = \frac{p_{\text{goal}} - p_i}{\|p_{\text{goal}} - p_i\|} - v_i$ where $p_{\text{goal}} = [0, 100]^T$. The system aimed to maintain strong 3-robustness to achieve consensus under a 1-local malicious attack. Fig. 2 and 3 depict the robots' trajectories in their LED colors and consensus values, respectively. In both environments, the system maintained strong 3-robustness, and normal followers matched their LED colors to those of the normal leaders.

	Env. 1	Env. 2
Baseline 1	47.65 (Failed 36 times)	45.57 (Failed 18 times)
Baseline 2	13.46	12.42
Ours	11.72	11.82

TABLE I: Time (in seconds) for controllers to reach exits in two environments from Fig. 2. For Baseline 1, we record the average performance of successful trials out of 50 attempts with randomly generated topologies. Trials with $t \geq 50$ were considered failures.

3) Comparisons: To demonstrate the flexibility of our CBF in network formation, we compared its performance with two other CBFs: Baseline 1 that maintains fixed topologies as in [33] and Baseline 2 from [16]. For each, we measured the time for all robots to reach the exits in two environments (Fig. 2) while maintaining strong 3-robustness. Although Baseline 2 focuses on r -robustness which does not extend to strong r -robustness [8], [15], we included it to maintain 3-robustness for a more comprehensive comparison. For fairness, all comparisons were conducted with 1) the same parameters, 2) single integrator dynamics, as in [16], [33], and 3) a centralized CBF-QP controller setup. A more flexible controller should lead to shorter exit times. Table I displays the recorded times. Trials with $t \geq 50$ were considered failures. Baseline 1 was evaluated based on the average performance of successful trials across 50 attempts. Each trial used strongly 3-robust Erdős–Rényi random graphs [36], [37] with $n = 15$ nodes and an edge probability of 0.3. Table I shows our CBF allowed the robots to reach the exits fastest in both environments, significantly outperforming Baseline 1. This illustrates that our approach offers greater flexibility in maintaining strong r -robustness.

B. Hardware Experiment

We illustrate practical application of our method using Crazyflie (CF) 2.0 platform. Our setup consisted of eight CFs: four normal leaders and four followers (one malicious). Initially arranged to form a strongly 4-robust network with a communication range of $R = 2.5$ m, the CFs were to maintain strong 3-robustness throughout the experiments. We used the Crazyswarm 1.0 ROS Neotic package [38] along with two Crazyradio PAs for communication and 15 Vicon motion capture cameras for localization. Control inputs were computed offboard by solving QP (29) on a computer and sent to each CF. To prevent trivial formations where drones vertically align or fly at high altitudes to avoid obstacles, we fixed their altitudes at 0.7m. We tested our proposed CBF on hardware by replicating the simulation scenarios. In the first scenario, we set $p_{i,\text{goal}}$ in (30) such that four leaders would spread out in different directions. The next two experiments involved environments similar to Fig.2 with 1) a narrow space and 2) multiple obstacles of varying sizes. In all cases, the drones successfully maintained strong 3-robustness, and normal followers successfully matched their LED colors to those of normal leaders. Due to space constraints, results and videos are available here¹.

VII. CONCLUSION

This paper presents a Control Barrier Function (CBF) that guarantees the maintenance of a multi-robot network's strong r -robustness above some threshold. We construct a valid CBF by composing multiple HOCBFs, each of which addresses an agent's sufficient connectivity for the network's robustness. Our approach directly considers robustness without predetermined topologies, thus offering greater flexibility in network formation. We have evaluated our method with simulations and hardware experiments.

REFERENCES

- [1] H. Zhu, J. Juhl, L. Ferranti, and J. Alonso-Mora, "Distributed multi-robot formation splitting and merging in dynamic environments," in *2019 International Conference on Robotics and Automation (ICRA)*, 2019, pp. 9080–9086.
- [2] K. B. Naveed, A. Dang, R. Kumar, and D. Panagou, "mesch: Multi-agent energy-aware scheduling for task persistence," 2024. [Online]. Available: <https://arxiv.org/abs/2406.04560>
- [3] P. Zhang, H. Xue, S. Gao, and J. Zhang, "Distributed adaptive consensus tracking control for multi-agent system with communication constraints," *IEEE Transactions on Parallel and Distributed Systems*, vol. 32, no. 6, pp. 1293–1306, 2021.
- [4] J. Usevitch and D. Panagou, "Resilient leader-follower consensus to arbitrary reference values in time-varying graphs," *IEEE Transactions on Automatic Control*, vol. 65, pp. 1755–1762, 2020.
- [5] W. Ren, "Consensus tracking under directed interaction topologies: algorithms and experiments," *IEEE Transactions on Control Systems Technology*, vol. 18, pp. 230–237, 2010.
- [6] J. Usevitch and D. Panagou, "Resilient trajectory propagation in multirobot networks," *IEEE Transactions on Robotics*, vol. 38, no. 1, pp. 42–56, 2022.
- [7] D. V. Dimarogonas, P. Tsiotras, and K. J. Kyriakopoulos, "Leader-follower cooperative attitude control of multiple rigid bodies," in *2008 American Control Conference*, 2008, pp. 801–806.
- [8] H. Rezaee, T. Parisini, and M. M. Polycarpou, "Resiliency in dynamic leader-follower multiagent systems," *Automatica*, vol. 125, p. 109384, 2021.
- [9] H. J. LeBlanc, H. Zhang, X. Koutsoukos, and S. Sundaram, "Resilient asymptotic consensus in robust networks," *IEEE Journal on Selected Areas in Communications*, vol. 31, no. 4, pp. 766–781, 2013.
- [10] D. Saldaña, A. Prorok, S. Sundaram, M. F. M. Campos, and V. Kumar, "Resilient consensus for time-varying networks of dynamic agents," in *2017 American Control Conference (ACC)*, 2017, pp. 252–258.
- [11] W. Abbas, A. Laszka, and X. Koutsoukos, "Improving network connectivity and robustness using trusted nodes with application to resilient consensus," *IEEE Transactions on Control of Network Systems*, vol. 5, no. 4, pp. 2036–2048, 2018.
- [12] J. Li, X. Dong, J. Yu, Q. Li, and Z. Ren, "Resilient time-varying formation tracking for heterogeneous high-order multiagent systems with multiple dynamic leaders," *IEEE Transactions on Control of Network Systems*, vol. 11, no. 1, pp. 89–100, 2024.
- [13] A. Mitra and S. Sundaram, "Byzantine-resilient distributed observers for lti systems," *Automatica*, vol. 108, p. 108487, 2019.
- [14] H. Lee and D. Panagou, "Construction of the sparsest maximally r -robust graphs," in *2024 IEEE 63rd Conference on Decision and Control (CDC)*, 2024, pp. 170–177.
- [15] J. Usevitch and D. Panagou, "Resilient leader-follower consensus to arbitrary reference values," *2018 Annual American Control Conference (ACC)*, 2018.
- [16] M. Cavorsi, B. Capelli, and S. Gil, "Multi-robot adversarial resilience using control barrier functions," *Robotics: Science and Systems*, 2022.
- [17] K. Saulnier, D. Saldaña, A. Prorok, G. J. Pappas, and V. Kumar, "Resilient flocking for mobile robot teams," *IEEE Robotics and Automation Letters*, vol. 2, pp. 1039–1046, 2017.
- [18] L. Guerrero-Bonilla and V. Kumar, "Realization of r -robust formations in the plane using control barrier functions," *IEEE Control Systems Letters*, vol. 4, no. 2, pp. 343–348, 2020.
- [19] M. Pirani, A. Mitra, and S. Sundaram, "Graph-theoretic approaches for analyzing the resilience of distributed control systems: A tutorial and survey," *Automatica*, vol. 157, p. 111264, 2023.
- [20] A. Ames, S. D. Coogan, M. Egerstedt, G. Notomista, K. Sreenath, and P. Tabuada, "Control barrier functions: Theory and applications," *2019 18th European Control Conference (ECC)*, pp. 3420–3431, 2019.
- [21] A. D. Ames, X. Xu, J. W. Grizzle, and P. Tabuada, "Control barrier function based quadratic programs for safety critical systems," *IEEE Transactions on Automatic Control*, vol. 62, pp. 3861–3876, 2017.
- [22] K. Garg, J. Usevitch, J. Breeden, M. Black, D. Agrawal, H. Parwana, and D. Panagou, "Advances in the theory of control barrier functions: Addressing practical challenges in safe control synthesis for autonomous and robotic systems," *Annual Reviews in Control*, vol. 57, p. 100945, 2024. [Online]. Available: <https://www.sciencedirect.com/science/article/pii/S1367578824000142>
- [23] T. Kim and D. Panagou, "Visibility-aware rrt* for safety-critical navigation of perception-limited robots in unknown environments," 2024. [Online]. Available: <https://arxiv.org/abs/2406.07728>
- [24] D. R. Agrawal and D. Panagou, "Safe and robust observer-controller synthesis using control barrier functions," *IEEE Control Systems Letters*, vol. 7, pp. 127–132, 2023.
- [25] W. Xiao and C. Belta, "High-order control barrier functions," *IEEE Transactions on Automatic Control*, vol. 67, no. 7, pp. 3655–3662, 2022.
- [26] T. Kim, R. I. Kee, and D. Panagou, "Learning to refine input constrained control barrier functions via uncertainty-aware online parameter adaptation," in *2025 IEEE International Conference on Robotics and Automation (ICRA)*, 2025.
- [27] C. Dawson, Z. Qin, S. Gao, and C. Fan, "Safe nonlinear control using robust neural lyapunov-barrier functions," in *Proceedings of the 5th Conference on Robot Learning*, ser. Proceedings of Machine Learning Research, A. Faust, D. Hsu, and G. Neumann, Eds., vol. 164. PMLR, 08–11 Nov 2022, pp. 1724–1735. [Online]. Available: <https://proceedings.mlr.press/v164/dawson22a.html>
- [28] W. Xiao, T.-H. Wang, R. Hasani, M. Chahine, A. Amini, X. Li, and D. Rus, "BarrierNet: Differentiable control barrier functions for learning of safe robot control," *IEEE Transactions on Robotics*, vol. 39, no. 3, pp. 2289–2307, 2023.
- [29] W. Ren and E. Atkins, "Distributed multi-vehicle coordinated control via local information exchange," *International Journal of Robust and Nonlinear Control*, vol. 17, no. 10-11, pp. 1002–1033, 2007. [Online]. Available: <https://onlinelibrary.wiley.com/doi/abs/10.1002/rnc.1147>
- [30] S. Janson, T. Łuczak, T. S. Turova, and T. Vallier, "Bootstrap percolation on the random graph $g_{n,p}$," *The Annals of Applied Probability*, vol. 22, 2012.
- [31] B. Capelli and L. Sabattini, "Connectivity maintenance: Global and optimized approach through control barrier functions," in *2020 IEEE International Conference on Robotics and Automation (ICRA)*, 2020, pp. 5590–5596.
- [32] M. Black and D. Panagou, "Adaptation for validation of consolidated control barrier functions," in *2023 62nd IEEE Conference on Decision and Control (CDC)*, 2023, pp. 751–757.
- [33] M. Egerstedt, J. N. Pauli, G. Notomista, and S. Hutchinson, "Robot ecology: Constraint-based control design for long duration autonomy," *Annual Reviews in Control*, vol. 46, pp. 1–7, 2018. [Online]. Available: <https://www.sciencedirect.com/science/article/pii/S136757881830141X>
- [34] P. Glotfelter, J. Cortés, and M. Egerstedt, "Nonsmooth barrier functions with applications to multi-robot systems," *IEEE Control Systems Letters*, vol. 1, no. 2, pp. 310–315, 2017.
- [35] J. Breeden and D. Panagou, "Compositions of multiple control barrier functions under input constraints," in *2023 American Control Conference (ACC)*, 2023, pp. 3688–3695.
- [36] P. Erdős and A. Rényi, "On the strength of connectedness of a random graph," *Acta Mathematica Academiae Scientiarum Hungaricae*, vol. 12, pp. 261–267, 1964.
- [37] B. Bollobás, *Random Graphs*, 2nd ed., ser. Cambridge Studies in Advanced Mathematics. Cambridge University Press, 2001.
- [38] J. A. Preiss*, W. Hönig*, G. S. Sukhatme, and N. Ayanian, "Crazyswarm: A large nano-quadcopter swarm," in *IEEE International Conference on Robotics and Automation (ICRA)*. IEEE, 2017, pp. 3299–3304, software available at <https://github.com/USC-ACTLab/crazyswarm>. [Online]. Available: <https://doi.org/10.1109/ICRA.2017.7989376>